ELSEVIER

Biophysical Chemistry 131 (2007) 1 – 14

Biophysical Chemistry

http://www.elsevier.com/locate/biophyschem

# Sequence and length dependent thermodynamic differences in heterocyclic diamidine interactions at AT base pairs in the DNA minor groove

Yang Liu, Arvind Kumar, David W. Boykin, W. David Wilson *

*Department of Chemistry, Georgia State University, Atlanta, GA 30302-4098, USA*

Received 18 July 2007; received in revised form 22 August 2007; accepted 23 August 2007
Available online 6 September 2007

**Abstract**

With the goal of developing a better understanding of the antiparasitic biological action of DB75, we have evaluated its interaction with duplex alternating and nonalternating sequence AT polymers and oligomers. These DNAs provide an important pair of sequences in a detailed thermodynamic analysis of variations in interaction of DB75 with AT sites. The results for DB75 binding to the alternating and nonalternating AT sequences are quite different at the fundamental thermodynamic level. Although the Gibbs energies are similar, the enthalpies for DB75 binding with poly(dA)·poly(dT) and poly(dA-dT)·poly(dA-dT) are +3.1 and −4.5 kcal/mol, respectively, while the binding entropies are 41.7 and 15.2 cal/mol·K, respectively. The underlying thermodynamics of binding to AT sites in the minor groove plays a key role in the recognition process. It was also observed that DB75 binding with poly(dA)·poly(dT) can induce T·A·T triplet formation and the compound binds strongly to the dT·dA·dT triplex.
© 2007 Elsevier B.V. All rights reserved.

*Keywords:* DB75; Alternating and nonalternating AT DNAs; Thermodynamics; Differential scanning calorimetry; Isothermal titration microcalorimetry; Biosensor-surface plasmon resonance

## 1. Introduction

Synthetic organic cations that bind to the DNA minor groove provide important examples of clinically useful therapeutic agents, biotechnology regents and compounds to probe the molecular basis of DNA recognition and control gene expression. Investigations on the molecular basis of DNA minor groove recognition by a variety of agents over the last several years have produced some interesting and thought-provoking results. As shown by DNA footprinting methods, well-characterized and structurally-diverse compounds, such as netropsin, Hoechst 33258 and berenil, which bind at AT sites in the DNA minor groove, can interact with a large variety of AT sequences [1,2]. For compounds of this size, a site of at least four base pairs in length is required but the affinities of the compounds for different AT sites can vary by a surprisingly large amount [3–5]. Early studies of netropsin binding to synthetic polydeoxyribonucleotides by Zimmer and coworkers [6,7] revealed sequence dependent differences in affinities and complex structures. The weak binding of the minor groove-targeted compounds listed above to GC containing sites has been explained by structural studies which show the compounds bound deep in the minor groove in AT sites and in close contact with the edges of AT base pairs at the floor of the groove [8–12]. This allows H-bonds to form with the TO2 and AN3 groups in AT base pairs but such close contact is sterically prevented by the 2-$NH_2$ group of G. The diversity of affinities for minor groove compounds with AT sequences, however, has not been extensively investigated.

The importance of the G–$NH_2$ group for binding specificity was verified by Bailly and Waring [13] who showed that replacement of G by inosine and substitution of 2,6-diaminopurine (DAP) for adenosine completely reversed the AT/GC binding specificity of minor groove binding agents. Fox and coworkers [4] conducted a detailed footprinting study with netropsin, Hoechst 33258 and berenil with a designed DNA sequence that contained all possible sequences of four AT base pairs. The largest variations in affinity were found in comparison of sites such as

*Abbreviations:* ITC, isothermal titration microcalorimetry; DSC, differential scanning calorimetry; SPR, surface plasmon resonance; CD, circular dichroism; Tm, thermal melting; kDNA, kinetoplast DNA; MES, 2-(*N*-morpholino) ethanesulfonic acid; RU, response units.

* Corresponding author. Tel.: +1 404 413 5503; fax: +1 404 413 5505.
*E-mail address:* wdw@gsu.edu (W.D. Wilson).

0301-4622/$ - see front matter © 2007 Elsevier B.V. All rights reserved.
doi:10.1016/j.bpc.2007.08.007

AATT, which binds all three ligands quite strongly, and sites with a TA step such as TATA and TTAA, which bind the ligands significantly more weakly. With Hoechst 33258, for example, there is a fifty fold decrease in binding from the AATT to the TATA site [4]. Footprinting results with the AAAA and ATAT sequences, which are the same as in the synthetic polymers, poly (dA)·poly(dT) and poly(dA-dT)·poly(dA-dT), vary significantly among the compounds. Hoechst 33258 binds approximately ten fold better to the $A_4$ sequence, netropsin binds approximately three times better to that sequence but berenil shows no significant difference in affinity between the alternating and nonalternating sites. Berenil does bind at least ten fold more weakly to TTAA than to AATT, however, and it is clear that all of the minor groove binding compounds have different abilities to distinguish among equivalent length AT binding sequences [4].

Breusegem et al. [14], by using fluorescence changes on binding, found a 200 fold better affinity for Hoechst 33258 binding to AATT versus TTAA in DNA oligomers while a 30 fold difference was observed for the heterocyclic diamidine, DAPI, with the same sequences. It has been suggested that the difference among these sites is at least partly due to differences in groove width [15–17]. Sites such as AATT, for example, have a more narrow groove than TTAA and are in a prebinding conformation that is better suited to complex formation with unfused heterocyclic compounds such as those discussed above. There are, no doubt, other contributing factors that result in individual compound differences, such as groove hydration and local sequence dependent helix axis bending [18].

Heterocyclic diamidines that target AT sequences and that have significant biological activity against specific DNA target sites in parasitic microorganisms [19–21] are of particular interest for drug development. A prodrug of the lead compound, DB75 (Fig. 1), is currently in phase III clinical trials against trypanosome induced sleeping sickness and other compounds of this type are being tested against trypanosomes and other diseases in humans [19,22]. For detailed understanding of the biological mechanism of the diamidines as well as for drug design and development progress, it is important to develop a thorough understanding of the molecular recognition of different DNA sequences by these compounds. The underlying thermodynamics of binding to AT sites in the minor groove can be quite different and can play a key role in the recognition process. Leng and coworkers [23] have recently shown, for example, that the AT-hook transcription factor, HMGA, which targets AT sites in the DNA minor groove, has similar Gibbs energy for binding to alternating and nonalternating AT sites but quite different enthalpies of binding. Examples of enthalpy/entropy compensation have also been observed with minor groove binding drugs and different DNA AT sites. Binding of netropsin to poly(dA-dT)·poly(dA-dT), for example, is enthalpy driven but the binding to poly(dA)·poly(dT) is driven by entropy [24,25].

Diamidine compounds, such as DB75, have been shown to specifically target AT rich DNA sequences, such as those in the trypanosome mitochondrial kinetoplast DNA, and this can result in differential biological activities or cell type targeting. The kinetoplast DNA (kDNA) has been shown by fluorescence

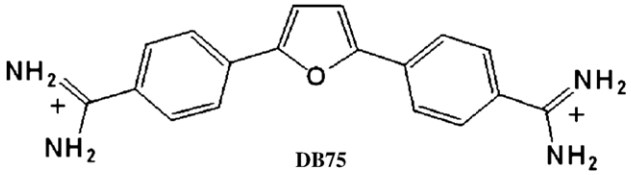


poly(dA)·poly(dT): $dA_n \cdot dT_n$

poly(dA-dT)·poly(dA-dT): $d(AT)_n \cdot d(AT)_n$

A15 Hairpin: 5'– $CCA_{15}GC$ C / $GGT_{15}CG$ C C

5'– Biotin $CCA_{15}GC$ C / $GGT_{15}CG$ C C

(AT)7 Hairpin: 5'– $CC(AT)_7AGC$ C / $GG(TA)_7TCG$ C C

5'– Biotin $CC(AT)_7AGC$ C / $GG(TA)_7TCG$ C C

A8 Hairpin: 5'– $CAAAAAAAA$ C / $GTTTTTTTT$ C C

(AT)4 Hairpin: 5'– $CATATATAT$ C / $GTATATATA$ C C

(CG)4 Hairpin: 5'– Biotin $CGCGCGCG$ T / $GCGCGCGC$ T T

Fig. 1. Structure of the compound and the DNA sequences used in this study.

microscopy studies to be the favored binding site of the compounds [22]. The kDNA is one of the most unusual nucleic acid structures found in any organism [26–28]. In *T. brucei*, the cause of sleeping sickness, the structure consists of approximately 50 DNA maxicircles of 20,000–40,000 base pairs. These are the coding DNAs of the mitochondria and are similar to the mitochondrial genomes of other organisms. There are approximately 10,000 minicircles of 1000 base pairs that are interlinked with the maxicircles to form a disk-shaped kinetoplast. The minicircles are AT rich, typically 70–75% AT base pairs, and contain phased A-tracts that lead to significant bending of the DNA helix. The extensive AT sequences in the minicircle DNAs form an attractive target for AT specific DNA binding compound. Even a small amount of interference with transcription and replication of minicircles can cause specific destruction of the complex interlocked kinetoplast structure and death of the trypanosome cell. A-tract bent DNA was discovered in early studies of minicircle DNAs from both trypanosome and Leishmania cells. DNA sequences for 25 minicircles have been reported and compared recently [29]. The minicircles contain nearly 100 AT sites of four or more contiguous AT base pairs that are potential binding receptor sites for diamidine drugs such as DB75 (Fig. 1). Clearly, to better understand the mechanism of action of the diamidines against kinetoplastid parasites and to design a broader range of improved drugs, it is essential to investigate the interaction of diamidines, such as DB75, with DNAs of different AT sequences.

With the goal of developing a better understanding of the antiparasitic biological action of DB75 as well as to better understand the molecular recognition of DNA by this biologically important compound, we have evaluated its interaction with the duplex alternating and nonalternating sequence AT polymers and oligomers. These DNAs provide an important pair of sequences of an initial detailed analysis of variations in interaction of DB75 with AT sites of different sequence. Although the primary method used in the studies is isothermal titration calorimetry (ITC), results for ultraviolet thermal melting (Tm), circular dichroism (CD), biosensor-surface plasmon resonance (SPR) and differential scanning calorimetry (DSC) are also presented. The results for DB75 binding to the alternating and nonalternating AT sequences are quite different at the fundamental thermodynamic level. Because kinetoplast DNAs are closed circles with extended A-tracts, the possibility of fold back triple-helical structures is significant and we have, therefore conducted a limited study of DB75 binding to the triple-helical polymer composed of T·A·T triplets. We observed that DB75 can induce and bind strongly to the triplex complementary to those results reported by Chaires et al. [30] for several diamidines.

## 2. Materials and methods

### 2.1. Compound, DNAs, and buffers

DB75 was synthesized as previously described [31]. Its purity was verified by NMR and elemental analysis. The double stranded polymers poly(dA)·poly(dT), poly(dA-dT)·poly(dA-dT) were purchased from Pharmacia (U.S.A.), and used for spectroscopic and calorimetric experiments. The hairpin oligomers used in this study were $A_{15}$ [d(CCAAAAAAAAAAAAAAGCCCCCGCTTTTTTTTTTTTTTTGG)], $(AT)_7$ [d(CCATATATATATATATAGCCCCCGCTATATATATATATATGG], $A_8$ [d(CAAAAAAAACCCCTTTTTTTTG)] and $(AT)_4$ [d(CATATATATCCCCATATATATG)], with the hairpin loop sequences underlined. In SPR experiments, three 5′-Biotin labeled hairpin DNA oligomers namely d(Biotin-CCA$_{15}$GCCCCCGCT$_{15}$GG) ($A_{15}$ hairpin), d(Biotin-CATATATATATATATACCCCTATATATATATATG) [$(AT)_7$ hairpin], d(Biotin-CGCGCGCGTTTTCGCGCGCG) [$(CG)_4$ hairpin] were used. The above hairpin oligomers are all from Integrated DNA Technologies, Inc. with reverse phased HPLC purification and mass spectrometry characterization. The MES buffers used in these experiments contained 0.01 M [2-(*N*-morpholino) ethanesulfonic acid] (MES), 0.001 M EDTA, 0.1 M NaCl, pH 6.25.

### 2.2. UV melting studies

Ultraviolet melting curves were determined in 1 cm path length quartz cells using a Cary 300 UV–Visible spectrophotometer (Varian Inc., Palo Alto, CA), equipped with a thermoelectric temperature controller. Absorbance versus temperature profiles were measured at 260 nm with a heating rate of 0.5 °C/min. Experiments were generally conducted at a concentration of $4\times10^{-5}$ M base pairs for polymeric DNA and $1.5\times10^{-6}$ M oligomers for hairpin DNA. Thermal melting experiments for the DNA–compound complexes were conducted as a function of different ratios. Melting temperature ($T_m$) was taken as the temperature of half-dissociation of the DNA duplex or hairpin and was obtained from the maximum of the first derivative $dA/dT$ plots (where $A$ is absorbance and $T$ is temperature).

### 2.3. CD titration and melting studies

CD spectra were recorded using a Jasco J-810 instrument with a 1 cm cell and a scan speed of 50 nm/min with a response time of 1 s. The spectra from 500 to 220 nm were averaged over five scans. A buffer baseline scan was collected in the same cuvette and subtracted from the average scan for each sample. For isothermal titration studies, measurements were performed at 25 °C. The desired ratios of compound to DNA were obtained by adding DB75 to the cell containing a constant amount of DNA. For melting studies, CD spectra were collected at different temperatures from 10 °C to 95 °C. The compound to the polymeric DNA base pairs ratio was chosen as 0.25 and 0.5. Data processing and plotting were performed with Kaleidagraph software.

### 2.4. DSC melting studies

The DSC experiments were performed on a Microcal VP-DSC microcalorimeter (MicroCal Inc., Northampton, MA, USA). The polymeric DNA [poly(dA)·poly(dT) or poly(dA-dT)·poly(dA-dT)] solution at a concentration of 0.04 mM base pairs in MES10 buffer was used for all experiments. Prior to scanning, the buffer and the samples were vacuum-degassed. The experiments over

the temperature range from 10 to 110 °C and a heating rate of 60 °C/h was used. Primary data were corrected by subtraction of a buffer–buffer baseline, normalized to the concentration of DNA (in base pairs) and further base line corrected. Data acquisition and analysis were performed with the Origin graphics software. The calorimetric enthalpy, $\Delta H_{cal}$, was determined by integration of the area enclosed by the transition curve and the pre/posttransition baseline, and the melting temperature, $T_m$, was determined as the midpoint of the melting transition.

The binding constants for the DB75 complexes with the poly(dA)·poly(dT) or poly(dA-dT)·poly(dA-dT) duplex could be calculated using a $T_m$ shift method and the following equation:

$$\Delta H_m\left(1/T_m^0 - 1/T_m\right) = R\,\ln\left(1 + K_{T_m}L\right)^{1/n} \quad (1)$$

where $T_m^0$ is the melting temperature of the DNA alone, $T_m$ is the meting temperature in the presence of saturating amounts of ligand, $\Delta H_m$ is the enthalpy of DNA melting (per mol bp) determined by DSC, $R$ is the gas constant, $K_{T_m}$ is the ligand binding constant at $T_m$, $L$ is the free ligand concentration and $n$ is the ligand site size [32–34].

The DNA binding constant of DB75 at lower temperatures was estimated by use of the van't Hoff equation:

$$R\ln\left(K/K_{T_m}\right) = -\Delta H_b\left(1/T - 1/T_m\right) \quad (2)$$

where $K$ is the DNA binding constant of DB75 at temperature $T$, and $\Delta H_b$ is the enthalpy of binding of DB75 to DNA determined by ITC at the corresponding temperature [35].

### 2.5. ITC thermodynamic studies

The ITC experiments were performed with a MicroCal VP-ITC (MicroCal Inc., Northampton, MA, USA) interfaced with a computer for instrument control and data collection with Origin 5.0 software. In a typical titration, 7 μl of a 0.08 mM DB75 solution in MES10 buffer was added every 300 s to a total of 40 injections to polymeric DNA [poly(dA)·poly(dT) or poly(dA-dT)·poly(dA-dT)] solution in the sample cell at 0.04 mM base pairs. The observed heat for each injection was determined by integration of the power peak area with respect to time. Blank titrations were conducted by injecting the compound into the sample cell containing only MES10 buffer under the same conditions. The corrected interaction heat was determined by subtracting the blank heat from that for the compound/DNA titration. The number of binding sites, equilibrium constants, binding enthalpy and entropy were obtained by fitting the corrected data to an appropriate binding model (see Results).

Binding enthalpies for different length of DNA hairpins [$A_{15}$, $A_8$, $(AT)_7$, $(AT)_4$] with DB75 were determined using the "model-free ITC" protocol to obtain multiple estimates of $\Delta H°$ and to avoid any possible fitting bias [35,36]. This protocol, which uses a high DNA concentration, ensures that all titrated drug is effectively bound after each addition. Specifically, a 0.03 mM hairpin DNA solution was loaded into the sample cell and a 0.15 mM DB75 solution in MES10 buffer was titrated into DNA. Usually 20 injections of 7 μl were done with 300 s between injections to ensure equilibration. The heat of reaction ($\Delta H$) was obtained by integration of the peaks after each injection. The dilution heats, determined by injecting drug solution into the same sample cell loaded with buffer alone, were subtracted from the $\Delta H$ value determined for titration into hairpin DNA to render a corrected value for the binding-induced enthalpy change.

### 2.6. Biosensor-SPR studies

SPR measurements were performed with a four-channel BIAcore 2000 optical biosensor system (BIAcore Inc.). 5′-biotin labeled DNA samples [$A_{15}$ hairpin, $(AT)_4$ hairpin and $(CG)_4$ hairpin] were immobilized onto streptavidin-coated sensor chips (BIAcore SA) as previously described [37]. Three flow cells were used to immobilize the DNA oligomer samples, while a fourth cell was left blank as a control. The SPR experiments were performed in filtered, degassed MES10 buffer with $5\times10^{-3}$% v/v Surfactant P20. Steady state binding analysis was performed with multiple injections of different compound concentrations over the immobilized DNA surface at a flow rate of 25 μl/min and 25 °C. Solutions of known ligand concentration were injected through the flow cells until a constant steady-state response was obtained. Compound solution flow was then replaced by buffer flow resulting in dissociation of the complex. The reference response from the blank cell was subtracted from the response in each cell containing DNA to give a signal (RU, response units) that is directly proportional to the amount of bound compound. The predicted maximum response per bound compound in the steady-state region ($RU_{max}$) was determined from the DNA molecular weight, the amount of DNA on the flow cell, the compound molecular weight, and the refractive index gradient ratio of the compound and DNA, as previously described [37,38]. The number of binding sites and the equilibrium constant were obtained from fitting plots of RU versus $C_{free}$. Binding results from the SPR experiments were fit with two- ($K_3$, $K_4=0$), three- ($K_4=0$) or four-site interaction models:

$$r = \left(K_1^* C_{free} + 2^* K_1^* K_2^* C_{free}^2 + 3^* K_1^* K_2^* K_3^* C_{free}^3 + 4^* K_1^* K_2^* K_3^* K_4^* C_{free}^4\right)/ \left(1 + K_1^* C_{free} + K_1^* K_2^* C_{free}^2 + K_1^* K_2^* K_3^* C_{free}^3 + K_1^* K_2^* K_3^* K_4^* C_{free}^4\right)$$

where $r$ represents the moles of bound compound per mole of DNA hairpin duplex, $K_1$, $K_2$, $K_3$, $K_4$ are macroscopic binding constants, and $C_{free}$ is the free compound concentration in equilibrium with the complex.

## 3. Results

### 3.1. UV melting studies

Relative stabilities of the compound–DNA complexes were evaluated by temperature-dependent UV absorbance measurements at 260 nm (Fig. 2 and Fig. S1 in Supplementary materials). Fig. 2a shows the profiles of thermally induced denaturation of the complexes formed with poly(dA)·poly(dT) and poly(dA-dT)·poly(dA-dT) in the absence and presence of DB75 at ratios of 0.25 and 0.5 compound per base pair. The similar observed large increases in melting temperature indicate

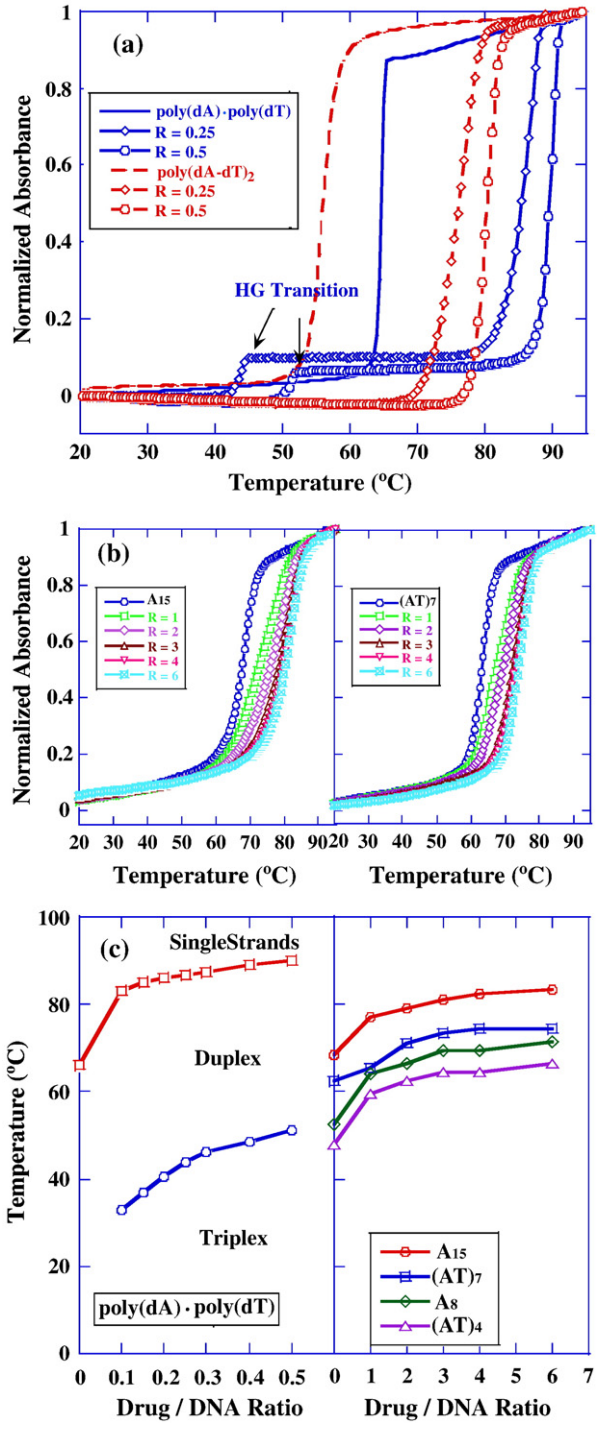


Fig. 2. UV melting profiles at 260 nm of the polymeric DNAs and DNA hairpins in the absence and presence of DB75. (a) Thermal melting curves of poly (dA)·poly(dT) and poly(dA-dT)·poly(dA-dT) at the indicated ratio of DB75 per base pair. (b) Thermal melting curves of A15 and AT7 hairpins at the indicated ratio of DB75 per oligomer. (c) A phase diagram for $T_m$ versus molar ratio for the thermal transitions of poly(dA)·poly(dT) (left) and DNA hairpins (right). The regions of triplex–duplex–single strand stability are labeled for the polymer. The oligomers have only duplex and single strand phase.

that DB75 binds strongly to both polymeric DNA samples. As can be seen, the melting profiles for poly(dA)·poly(dT) and poly(dA-dT)·poly(dA-dT) in the absence and presence of DB75 were significantly different in the low-temperature region. For the alternating copolymer duplex poly(dA-dT)·poly(dA-dT), the melting profiles in the absence and presence of DB75 were all monophasic, representing a single transition that corresponds to the well-known duplex to single strand denaturation of poly (dA-dT)·poly(dA-dT). In contrast, a biphasic melting profile was observed for poly(dA)·poly(dT) in the presence of DB75. The higher temperature transition corresponds to the melting of the expected Watson–Crick (WC) duplex, while the lower temperature transition is assigned to the dissociation of poly (dT) from poly(dA)·2poly(dT) triplex [the Hoogsteen (HG) transition] [30]. Without DB75 only the high-temperature WC transition for poly(dA)·poly(dT) was evident. Based on melting of a fully poly(dA)·2poly(dT) triplex (not shown), we estimate that there is approximately a 20% excess of the dT strand in the poly(dA)·poly(dT) duplex. The triplex formation suggests that the polymer sample contains a slight excess of the poly(dT) strand that can form a DB75 induced dT·dA·dT triplex under these conditions. The triplex formation is DNA sequence dependent as expected.

To investigate the effects of DB75 on inducing the triplex formation, UV melting experiments with poly(dA)·poly(dT) in the presence of increasing molar ratios of added DB75 were carried out (Fig. S1C, Supplementary materials). Upon addition of increasing molar ratios of DB75, two transitions were evident in melting profiles. These equilibrium positions are summarized with a triplex→duplex→single strand phase transition plot of thermal stability versus DB75 ratio in Fig. 2c (left). We observed significant effects of the DB75 ratio on the $T_m$ corresponding to the triplex to duplex transition, which increases from 32 °C to 51 °C, while that of duplex to single strand transition increases from 64 °C to 90 °C [Fig. 2c (left)] as the ratio is increased. These studies clearly show that triplex formation induced by DB75 binding is compound–DNA ratio and temperature-dependent.

The profiles of thermally induced denaturation of the complexes formed with DNA hairpins [$A_{15}$, $(AT)_7$, $A_8$ and $(AT)_4$), Fig. 1] in the absence and presence of DB75 at different ratios are shown in Fig. 2b and Fig. S1(A,B) (Supplementary materials). As expected, only one transition, corresponding to the unfolding of hairpin DNA, is observed in these melting profiles. The effect of DB75 ratio on the $T_m$ of DNA hairpins is shown in Fig. 2c (right). As can be seen, saturation binding is observed at compound–DNA ratios of 4:1 for $A_{15}$ and $(AT)_7$ hairpins, and 3:1 for $A_8$ and $(AT)_4$ hairpins.

### 3.2. CD titration and melting studies

CD titration experiments as a function of DB75 concentration were utilized to monitor the binding mode and saturation limit for DB75 complexes with poly(dA)·poly(dT) and poly (dA-dT)·poly(dA-dT) and DNA hairpins, $A_{15}$, $(AT)_7$, $A_8$ and $(AT)_4$ (Fig. 1). Results for the polymers in Fig. 3 show that the CD spectral titrations of DB75 had large positive induced CD signals above 300 nm for both AT sequences. In the 300–500 nm region, free DB75 and DNA do not exhibit CD signals. DNA does not absorb in this wavelength range and free DB75 is optically inactive. Positive CD signals arise from the interaction of the DB75 chromophore with the dissymmetric environment

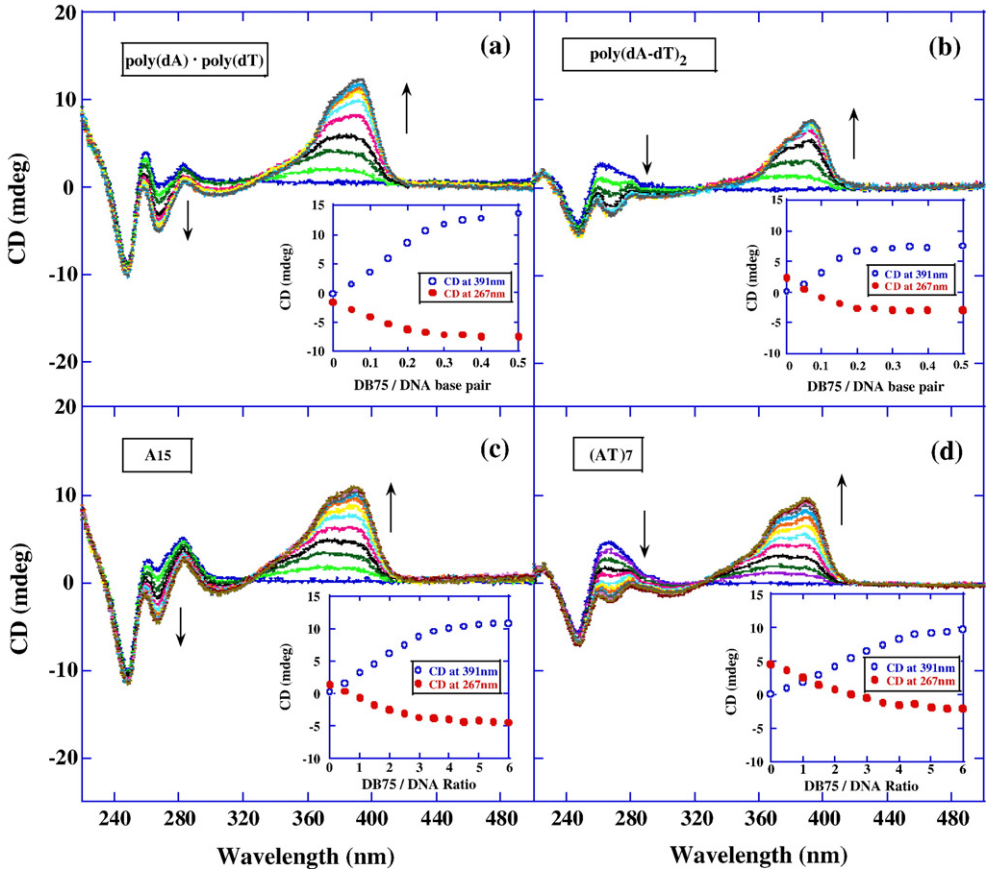


Fig. 3. CD titration spectra of the polymeric DNAs and DNA hairpins binding with DB75 at various mixing ratios. Insert: increase in CD magnitude at 391 nm (○) and decrease in CD magnitude at 267 nm (●).

of the DNA minor groove [39,40]. The large positive induced CD signal for the complex is a characteristic pattern for a minor grove binding mode in AT sequences. Similar CD patterns at 267 and 391 nm for poly(dA)·poly(dT) (Fig. 3a) and $A_{15}$ (Fig. 3c) as well as for poly(dA-dT)·poly(dA-dT) (Fig. 3b) and $(AT)_7$ (Fig. 3d) are also observed. The induced CD signals at 267 and 391 nm were also plotted against compound–DNA ratio (insert in Fig. 3). For the polymeric DNAs, the break in the plot at the ratio of ~0.25 indicates a binding site size of 4–5 base pairs DNA per compound, which agrees with the ITC results shown below. The saturated compound–DNA ratio obtained as 4 DB75/hairpin is also consistent with the UV melting (Fig. 2b) and SPR experiments (shown below).

To investigate the melting of the complexes formed by both polymeric DNAs in the absence and presence of DB75, the temperature-dependent CD spectra at various wavelengths were monitored (Fig. 4 and Fig. S3, Supplementary materials). In the presence of DB75 the CD melting curves of poly(dA)·poly(dT) at either 267 nm (Fig. 4a) or 391 nm (Fig. 4c) are clearly biphasic. In accordance with UV melting experiments, the lower temperature transition reflects dissociation of the poly (dT) third strand from the poly(dA)·2poly(dT) triplex (the HG transition), whereas the higher temperature transition corresponds to the expected WC dissociation reaction. These CD-detected transitions reaffirm that DB75 binding induced the formation of triple helices. As the DB75 ratio increases from 0.25 to 0.5, the $T_m$ for the HG and WC transition also increases, consistent with the UV melting experiments (Fig. 2a). In contrast to the biphasic melting profiles for poly(dA)·poly(dT), the CD melting curves of poly(dA-dT)·poly(dA-dT) were monophasic in the presence of DB75 at 267 nm (Fig. 4b) and 391 nm (Fig. 4d), indicating only a single WC transition.

### 3.3. DSC melting studies

DSC can be used to quantitatively evaluate thermally induced structural transitions in DNA. Binding of DB75 to poly(dA)·poly(dT) and poly(dA-dT)·poly(dA-dT) was evaluated from the DSC results by using a $T_m$ shift method (Fig. 5, Eq. (1)). The DSC enthalpy of DNA melting ($\Delta H_m$) and $T_m$ are shown in Table 1. Values for the $T_m$ in the presence and absence of DB75 are consistent in both UV melting and DSC experiments. In the presence of saturating concentrations of DB75, the $T_m$ increases 26 °C for poly(dA)·poly(dT) and 23 °C for poly(dA-dT)·poly(dA-dT), which agrees with strong binding for both polymeric DNAs. By application of Eqs. (1) and (2), described in Materials and methods, the binding constant ($K$) at 25 °C was calculated as $5.6\times10^6$ $M^{-1}$ for poly (dA)·poly(dT) and $5.4\times10^6$ $M^{-1}$ for poly(dA-dT)·poly(dA-dT), respectively. These equations require the enthalpy of binding of DB75 to the polymeric DNAs ($\Delta H_b$) at 25 °C and the ligand site size ($n$) determined by ITC, described below

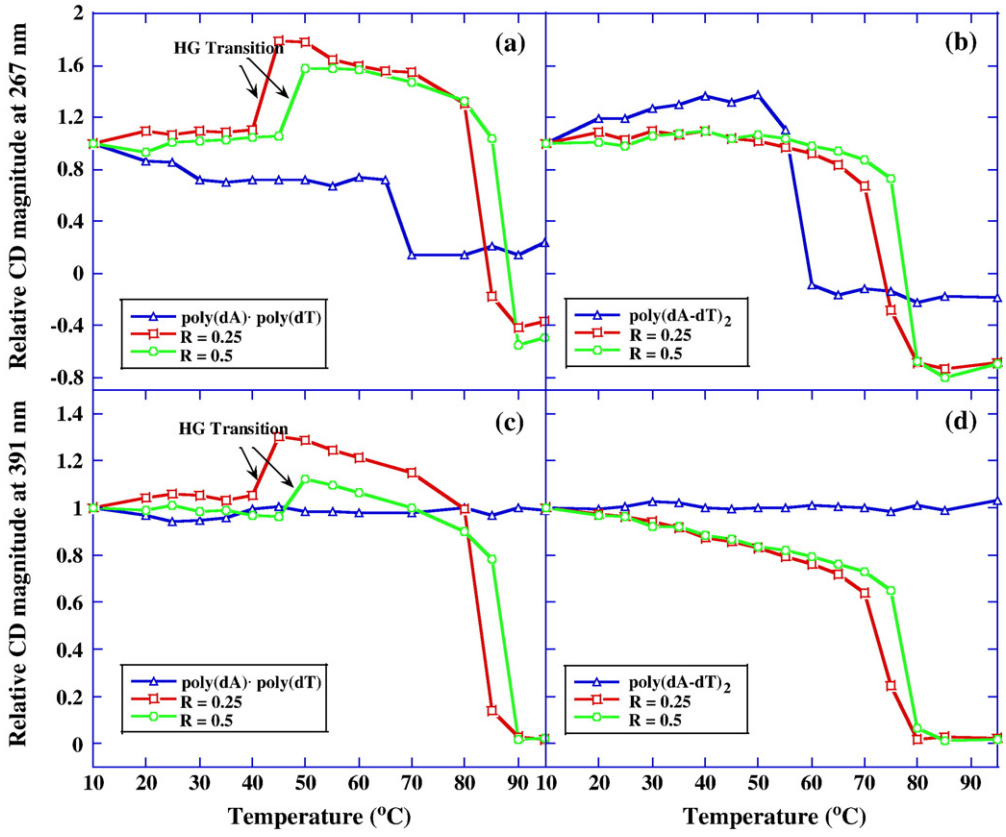


Fig. 4. Temperature-dependent CD magnitude (relative to the CD at 10 °C, $CD_T/CD_{10\ °C}$) of the polymeric DNAs and their DB75 complexes at 267 and 391 nm.

(Table 2). These $K$ values agree with the binding constants obtained from ITC experiments (Table 2). By using the above method, we could obtain $K$ at any temperature without assuming that $\Delta H_b$ is independent of temperature.

As observed in the UV and CD melting profiles (Figs. 2a and 4a), the heat capacity versus temperature curve for poly(dA)·poly(dT) binding with DB75 are also biphasic (Fig. 5a), with the low-temperature transition centered around 50 °C due to the dissociation of the poly(dT) third strand from the poly(dA)·2poly(dT) triplex (the HG transition) and the high-temperature transition at 90 °C due to the dissociation of the duplex strands (the WC transition). By contrast, a clear monophasic transition corresponding to WC transition appeared in the thermal denaturation profile for poly(dA-dT)·poly(dA-dT) binding with DB75 (Fig. 5b). The UV and CD melting profiles and the DSC thermograms for poly(dA)·poly(dT) all reveal triplex formation induced by DB75 binding.

### 3.4. ITC thermodynamic studies

To probe the detailed energetic basis of the DB75 sequence dependent interaction differences in more detail and at a constant temperature, ITC experiments were conducted with the AT sequence DNAs (Fig. 1). Calorimetric titration curves of poly(dA)·poly(dT) and poly(dA-dT)·poly(dA-dT) with DB75 at 25 °C (Fig. 6) are completely different. A large positive enthalpy is observed in the ITC titration of DB75 into poly(dA)·poly(dT), while a large negative enthalpy is obtained on titration of DB75 into alternating poly(dA-dT)·poly(dA-dT) at the same conditions. The titration heat was converted to heat per mole as a function of total molar ratio with subtraction of the heat for a blank titration of DB75 into buffer with no DNA. The corrected isotherm was fitted to a 1:1 model to obtain a full set of thermodynamic parameters (Table 2). The binding stoichiometry of 4–5 base pairs of DNA per compound by ITC experiments is consistent with that obtained from CD titration experiments. At 25 °C DB75 binding to poly(dA)·poly(dT) is overwhelmingly entropy driven, whereas DB75 binding to poly(dA-dT)·poly(dA-dT) is enthalpy driven. The similarity in the DB75 binding free energies for both polymeric DNAs results from impressive enthalpy–entropy compensation, a common signature of minor grove binders [41,42].

Binding enthalpies for different length DNA hairpins (Fig. 1) with DB75 were determined using a "model-free ITC" protocol at low binding ratios to avoid any fitting bias and influence by end effects for binding to oligomers [36]. Fig. 6c and d shows representative primary data from the titration of DB75 into $A_{15}$ and $(AT)_7$ hairpin DNA solution at 25 °C, respectively. As with polymeric DNAs, a large positive enthalpy was observed in ITC titration of DB75 into the $A_{15}$ hairpin and a large negative enthalpy for titration of DB75 into the alternating $(AT)_7$ hairpin. Integration of the peaks followed by normalization for the number of moles of added DB75 and subtraction of the blank heat provides a direct estimate of the binding enthalpy. The average binding enthalpy values are 2.9 kcal/mol for the $A_{15}$ hairpin and −4.6 kcal/mol for the $(AT)_7$ hairpin (Table 3).

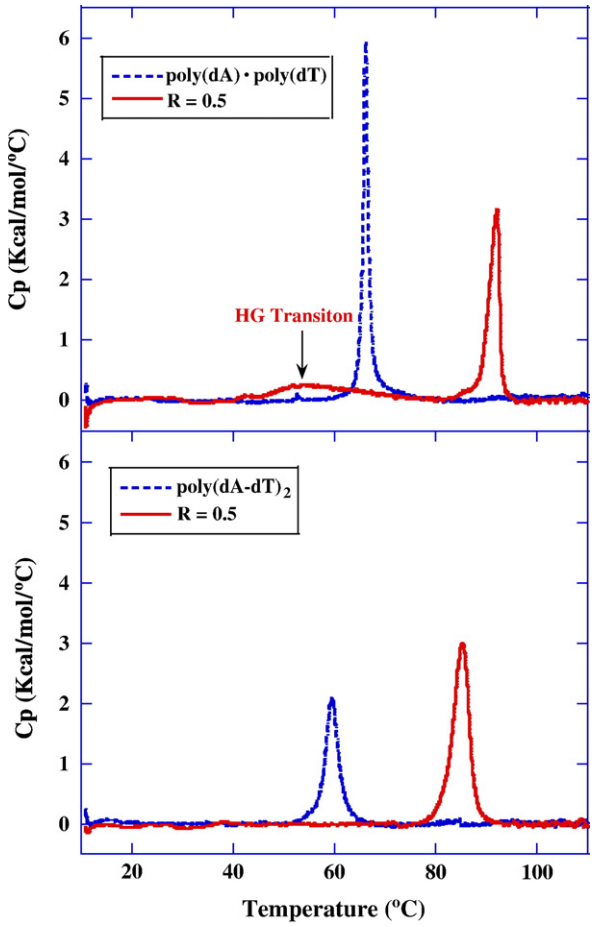


Fig. 5. DSC excess heat capacity ($\Delta C_p$) versus temperature profiles for polymeric DNAs binding with DB75. Melting curves for poly(dA)·poly(dT) in the absence and presence of DB75 (a), and poly(dA-dT)·poly(dA-dT) in the absence and presence of DB75 (b).

Interestingly, these values with the oligomer duplexes, closely match the endothermic and exothermic values for poly (dA)·poly(dT) and poly(dA-dT)·poly(dA-dT) (Table 2). The binding enthalpies for the still shorter $A_8$ and $(AT)_4$ hairpins with DB75, however, decreased relative to the polymers and 15mer hairpin sequences (Supplementary materials, Fig. S4). The average binding enthalpies are 0.064 kcal/mol for $A_8$ and −6.0 kcal/mol for $(AT)_4$, both substantially more negative than with the longer sequences. These results suggest that the $A_{15}$ and $(AT)_7$ hairpins are good models to mimic results with longer DNA binding sequences.

Table 1
DSC determined binding parameters for the interaction of DB75 with poly (dA)·poly(dT) and poly(dA-dT)·poly(dA-dT)[a]

| | $T_m^0$ (°C) | $T_m$ (°C) | $\Delta H_m$ (kcal/mol) | $K_{T_m}$ ($M^{-1}$) | $\Delta H_b$ (kcal/mol) | $K$ ($M^{-1}$) |
|---|---|---|---|---|---|---|
| Poly(dA)·poly(dT) | 66.1 | 92.2 | 9.84 | $1.82\times10^7$ | 3.11 | $6.94\times10^6$ |
| Poly(dA-dT)$_2$ | 59.5 | 82.4 | 7.16 | $1.57\times10^6$ | −4.52 | $5.35\times10^6$ |

[a] Experiments were carried out in MES10 buffer at 25 °C. The $\Delta H_m$ values are from DSC and $\Delta H_b$ values are from ITC. The $\Delta H$ values have an experimental error of approximately ±5%.

Table 2
ITC determined binding parameters for the interaction of DB75 with poly (dA)·poly(dT) and poly(dA-dT)·poly(dA-dT)[a]

| | $n$ (bp/drug) | $K$ ($M^{-1}$) | $\Delta H$ (kcal/mol) | $T\Delta S$ (kcal/mol) | $\Delta G$ (kcal/mol) | $\Delta C_p$ (cal $mol^{-1}$ $K^{-1}$) |
|---|---|---|---|---|---|---|
| Poly(dA)·poly (dT) | 4.71 | $7.06\times10^6$ | 3.11 | 12.4 | −9.34 | −174 |
| Poly(dA-dT)$_2$ | 4.01 | $4.51\times10^6$ | −4.52 | 4.54 | −9.06 | −127 |

[a] Experimental error limits for ITC experiments are approximately ±5%.

To investigate the sequence dependent binding differences for DB75 in more detail, the corrected binding isotherms for DB75 titrations into the two polymeric DNAs at different temperatures from 5 °C to 50 °C were obtained (Supplementary

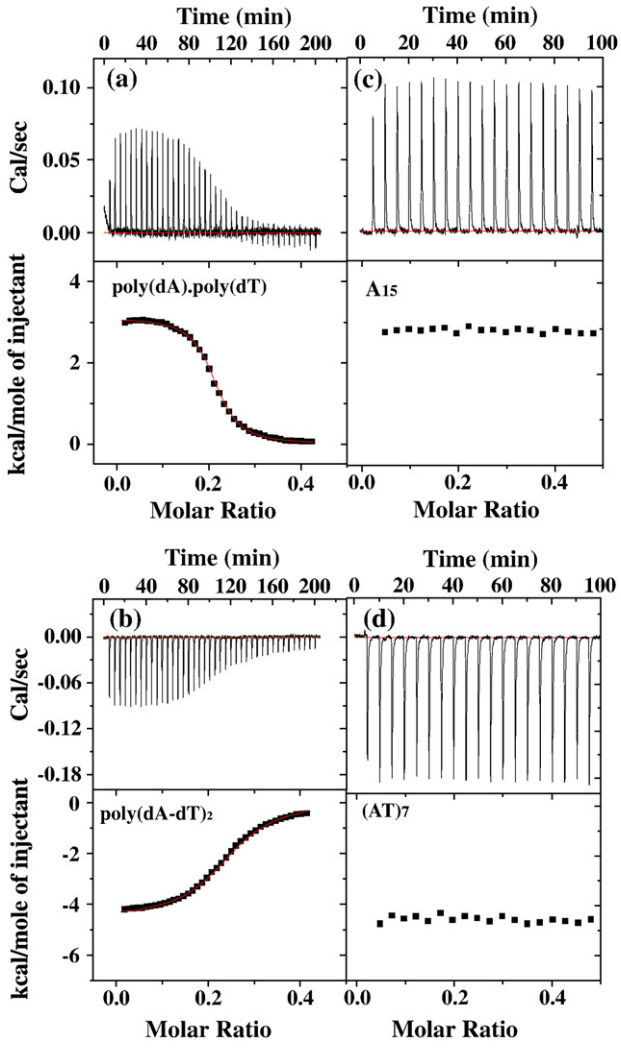


Fig. 6. ITC curves for the binding of DB75 to the AT DNA polymers and hairpins in MES10 at 25 °C. Every peak represents the instrument response for injection of DB75 into DNA during the course of the titration (top). A binding isotherm from integration with respect to time, with appropriate dilution correction (bottom). For poly(dA)·poly(dT) (a) and poly(dA-dT)·poly(dA-dT) (b), the smooth lines show the fit to the results and best fit $\Delta H$ (Table 2) values for binding. For $A_{15}$ (c) and $(AT)_7$ (d) hairpins, a 'model-free ITC' protocol was used to obtain $\Delta H$.

Table 3
SPR determined binding parameters for the interaction of DB75 with $A_{15}$, $(AT)_7$ and $(CG)_4$ sequences

| | $K_1$ ($M^{-1}$) | $K_2$ ($M^{-1}$) | $K_3$ ($M^{-1}$) | $K_4$ ($M^{-1}$) | $K_{mean}$ [a] ($M^{-1}$) | $\Delta G$ (kcal/mol) | $\Delta H$ [b] (kcal/mol) | $T\Delta S$ (kcal/mol) |
|---|---|---|---|---|---|---|---|---|
| $A_{15}$ | $2.99\times10^7$ | $2.95\times10^7$ | $2.34\times10^6$ | $1.91\times10^6$ | $1.59\times10^7$ | −9.81 | 2.94 | 12.8 |
| $(AT)_7$ | $5.09\times10^7$ | $4.61\times10^7$ | $3.79\times10^6$ | $8.40\times10^5$ | $2.54\times10^7$ | −10.08 | −4.56 | 5.52 |
| $(CG)_4$ | $2.14\times10^6$ | $2.63\times10^5$ | – | – | $1.20\times10^6$ | – | – | – |

Experimental error limits for SPR $K$ values and "model-free ITC" $\Delta H$ values are both approximately ±10%.
[a] $K_{mean}=(K_1+K_2+K_3+K_4)/4$.
[b] $\Delta H$ values are from "model-free ITC" experiments as described in Materials and methods.

materials, Fig. S5). Representative ITC titration and integrated heat results for the titration of DB75 into poly(dA)·poly(dT) and poly(dA-dT)·poly(dA-dT) at four different temperatures are plotted in Fig. 7. Inspection of Fig. S5A reveals that the binding enthalpies for poly(dA)·poly(dT) from 5 °C to 30 °C are strongly temperature-dependent and decrease regularly (becoming more exothermic) as the temperature is increased. At temperatures above 30 °C, however, we observed abnormal binding enthalpy drops, indicating that an unusual DNA conformation transition occurred. These drops at higher temperature are clearly DNA–compound ratio dependent. Previous UV melting experiments for poly(dA)·poly(dT) (Fig. 2c and Fig. S1C in Supplementary materials) showed that triplex formation induced by DB75 binding was DNA–compound ratio and temperature-dependent. The phase diagram in Fig. 2 suggests that we are observing a duplex–triplex transition at higher temperatures as DB75 is added to the duplex DNA.

Further inspection of Fig. S5B revealed that the binding enthalpies for poly(dA-dT)·poly(dA-dT) at all studied temperatures were negative and their magnitude decreased regularly with increasing temperature from 5 °C to 40 °C. When the temperature was above 45 °C, however, a larger, nonlinear decrease in binding enthalpy was observed. Since the $T_m$ for poly(dA-dT)·poly(dA-dT) itself was around 55 °C (Fig. 2a), it is likely that some premelted single strand DNA fractions fold back to poly(dA-dT)·poly(dA-dT) duplex on titration of DB75 into DNA solution at higher temperatures. In this case, the observed binding enthalpy is the sum of heat of binding interaction and heat of refolding DNA to give the abnormal large values relative to lower temperature results.

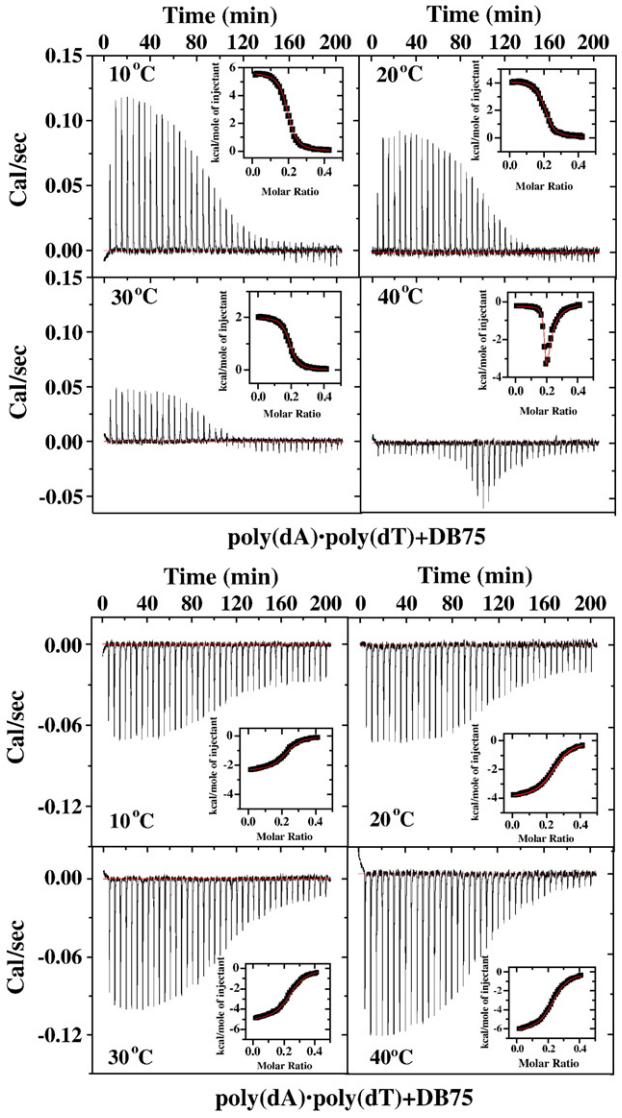


Fig. 7. Representative ITC titration and integrated heat data for DB75 binding to poly(dA)·poly(dT) (top) and poly(dA-dT)·poly(dA-dT) (bottom) at 10, 20, 30, 40 °C.

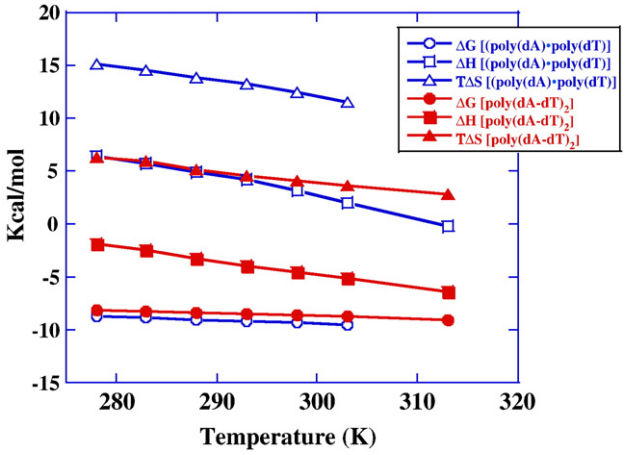


Fig. 8. Complete thermodynamic results for binding of DB75 to poly(dA)·poly(dT) (open) and poly(dA-dT)·poly(dA-dT) (solid) are shown as a function of temperature. Because the free energy changes much less with temperature than the enthalpy, there is significant enthalpy–entropy compensation as can be seen in the figure. The $\Delta C_p$ values in Table 2 are the slopes of the $\Delta H°$ plots and no curvature is apparent over this temperature range.

The corrected isotherms for poly(dA)·poly(dT) (from 5 °C to 30 °C) and poly(dA-dT)·poly(dA-dT) (from 5 °C to 40 °C) were fitted with 1:1 binding model to obtain the binding free energy, enthalpy and entropy (Fig. 8). Because the free energy values change much less with temperature than the enthalpies, there was a significant compensation in the enthalpy and entropy values as can be seen in Fig. 8. No curvature in the plots of the thermodynamic constants versus temperature is apparent over the corresponding temperature range and all of the plots were fitted with linear functions. The experimental heat capacity changes for formation of the complexes were obtained from linear fitting of binding enthalpy as a function of temperature (Table 2). The calculated $\Delta C_p$ values for DB75 binding are all large and negative: for poly(dA)·poly(dT), $-174\pm7.3$ cal $mol^{-1}K^{-1}$; for poly(dA-dT)·poly(dA-dT), $-127\pm3.1$ cal $mol^{-1}K^{-1}$.

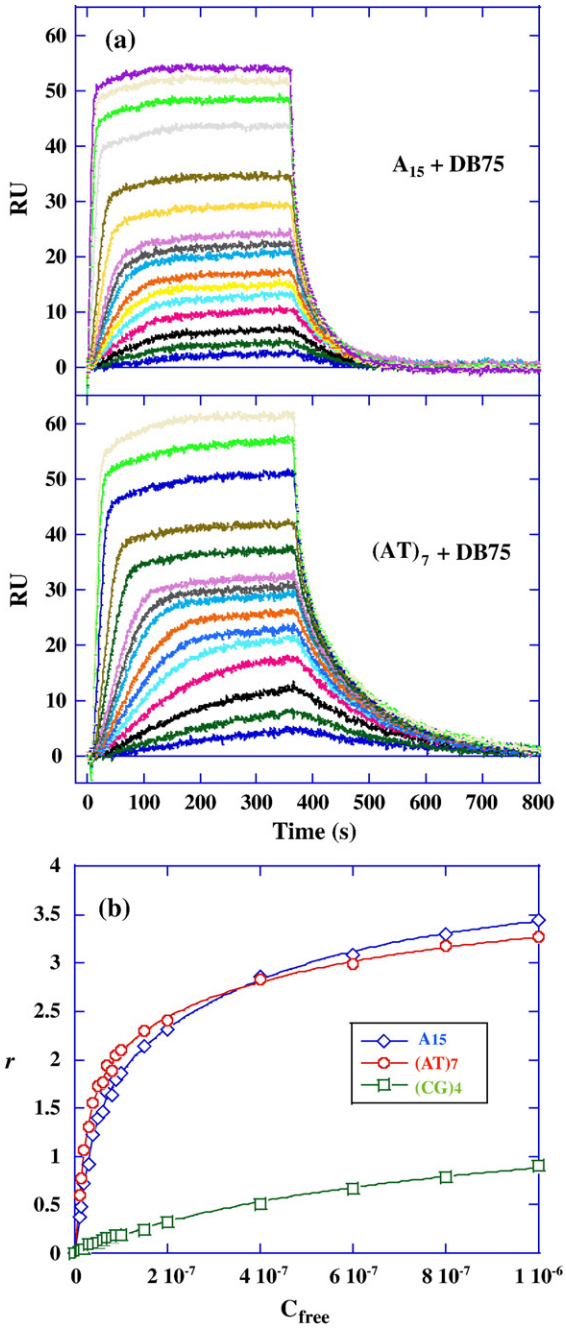


Fig. 9. SPR binding affinity: (a) SPR sensorgrams for the interaction of $A_{15}$ hairpin and $(AT)_7$ hairpin with DB75. The compound concentrations for DB75 from bottom to top are 0 to 1 μM. (b) RU values from the steady-state region of SPR sensorgrams were converted to $r$ ($r$=RU/$RU_{max}$) and are plotted against the unbound compound concentration (flow solution) for $A_{15}$ (diamonds), $(AT)_7$ (circles) and $(CG)_4$ (squares) hairpins binding with DB75. The lines are the best fit values using appropriate binding models.

### 3.5. Biosensor-SPR studies

Because large $K$ values are difficult to determine accurately at the concentrations generally required in diamidine–DNA ITC studies, the DB75–DNA binding constants were also evaluated by biosensor-SPR methods. Since ITC results show that the 15mer hairpins are good mimics for longer DNAs binding with DB75, 5′-Biotin labeled $A_{15}$, $(AT)_7$ and $(CG)_4$ hairpin sequences (Fig. 1) were immobilized on three flow cells of a Biacore sensor chip and the fourth flow cell was left blank for reference subtraction. Sensorgrams for the interaction of $A_{15}$ and $(AT)_7$ sequences with DB75 are compared in Fig. 9(a). The differences in interaction strength for all three sequences binding with DB75 could be more easily visualized in the plot of $r$ (moles of compound bound/mole of hairpin DNA) versus $C_{free}$, the free compound concentration [Fig. 9(b)]. The data for DB75 binding with $A_{15}$ and $(AT)_7$ hairpin are best fit with a four-site binding model and the $(CG)_4$ results were well fit using a two-site binding model (Table 3). As expected, DB75 binds strongly to $A_{15}$ and $(AT)_7$ hairpins with similar interaction strength, but it binds quite weakly to the $(CG)_4$ sequence. From $T_m$ melting (Fig. 2b) and CD titration experiments (Fig. 3c and d) of $A_{15}$ and $(AT)_7$ hairpins binding with DB75, the compound–DNA binding ratio of 4:1 was obtained. These observations are in good agreement with the SPR fitting results, suggesting that one $A_{15}$ or $(AT)_7$ sequence could bind four DB75 molecules. As described above, the average binding enthalpies for $A_{15}$ and $(AT)_7$ hairpins have been obtained using the model-free ITC protocol (Table 3). From the experimental binding free energy and enthalpy values, the entropies for $A_{15}$ and $(AT)_7$ hairpins could be calculated (Table 3).

## 4. Discussion

As described in the introduction, AT site specific minor groove binding diamidines are important for the development of new antiparasitic therapeutics and for biotechnology reagents. A prodrug of DB75, for example is in Phase III clinical trials against sleeping sickness [43] and a derivative of DB75 is the basis of a highly sensitive fluorescence assay for trypanosomes resistant to melarsoprol, the primary drug currently used to treat late stage sleeping sickness [44]. These compounds target the AT rich sequences of kDNA minicircles with destruction of the trypanosome kinetoplast and cell death [22].

In spite of extensive studies of diamidines as well as other AT specific minor groove agents, there is little quantitative information on the energetic basis for their ability to distinguish among different sequences in AT binding sites such as those in

kDNA. Available results for a small number of AT specific minor groove binding compounds indicate that binding affinities vary quite significantly among different sequences of all AT sites [4]. We have also discovered that similar variations can occur with sequence specific minor groove binding polyamides which recognize mixed sequences of DNA [45,46]. The polyamides have affinities for their cognate DNA binding sites, for example, that vary by over a factor of 1000. There are few detailed thermodynamic studies of the basis for the different affinities among minor groove binding sites. Given the increasing importance of diamidines as DNA-targeted therapeutics and biotechnology reagents, it is important to establish the variations in thermodynamic quantities that characterize their interactions at different sequence AT binding sites. Since a thermodynamic analysis of DB75 has been previously conducted with d $(CGCGAATTCGCG)_2$ [47] that compound has been used with the alternating and nonalternating DNA sequences of different length in the research reported here to probe the sequence dependent thermodynamics of binding. Since extended AT sequences in parasitic mitochondrial kinetoplast DNA have been shown to be the biological target of diamidines [22], these studies are part of the essential information needed for detailed understanding of the therapeutic activity of DB75 and for design of new drugs.

DB75 and a number of other diamidines have been crystallized with the self-complementary DNA duplex d $(CGCGAATTCGCG)_2$ [48]. The compounds bind in the minor groove at the -AATT- site and the complex is stabilized by H-bonding, van der Waals and electrostatic interactions. The curvature of DB75 lets it slide deeply into the minor groove and the twist of the diamidines allows them to H-bond with terminal T bases in the AATT sequences on opposite strands of the duplex [48]. In agreement with this binding mode, CD studies indicate that DB75 binds in a similar manner to the minor groove of the alternating and nonalternating AT sequences of different length (Fig. 3). Melting experiments by UV, CD and DSC methods all show that the alternating and nonalternating AT sites have similar affinities for DB75. Triple–helical dT·dA·dT is not stable under the conditions of these experiments but the melting studies also show that DB75 can induce formation of the triplex in the nonalternating sequence as the ratio of DB75 to duplex is increased. By using competition dialysis and melting experiments, Chaires et al. [30] previously have shown that DB75 is a triplex stabilizing agent.

SPR and ITC experiments confirm that DB75 has similar affinities for the alternating and nonalternating AT sequences, but ITC results illustrate striking differences in DB75 interactions with these two types of sites. At 25 °C, for example, the nonalternating sequence has $\Delta H$=+3.1 kcal/mol while the alternating sequence binds with an exothermic enthalpy of −4.5 kcal/mol. At the same temperature $\Delta H$=−2.2 kcal/mol for the AATT oligomer [47]. The three AT sequences have very similar binding Gibbs energies but they obtain the similar affinities with a large variation in the underlying thermodynamics of binding. Similar results with the AT polymers have been seen with other AT specific minor groove binding compounds such as netropsin [24,49].

To better understand the thermodynamics for DB75 binding with poly(dA)·poly(dT) and poly(dA-dT)·poly(dA-dT), the observed binding free energy ($\Delta G_{obs}$) at 25 °C for DB75 binding to DNA was divided into two primary contributions [50,51]:

$$\Delta G_{obs} = \Delta G_{pe} + \Delta G_t \quad (3)$$

where $\Delta G_{pe}$ is the electrostatic (polyelectrolyte) contribution, due mainly to coupled polyelectrolyte effects, the most important of which is the release of condensed counterions from the DNA helix upon ligand binding. $\Delta G_t$ is the nonpolyelectrolyte contribution, which arises from all other molecular interaction factors such as hydrophobic contacts, van der Waals forces, H-bonding, etc. The polyelectrolyte term may be calculated using the relationship [52]:

$$\Delta G_{pe} = Z^*\varphi^*\mathrm{RT}\ \ln\ (M^+) \quad (4)$$

where $Z$ is the charge on the ligand (for DB75, $Z$ is equal to 2 for the two amidines charged, Fig. 1), and $\phi$ is the proportion of total counterions associated with each DNA phosphate (about 0.88 for B-DNA duplex). $(M^+)$ is salt concentration. For both polymeric DNAs binding with DB75:

$$\Delta G_{pe} = 2^*0.88^*\mathrm{RT}\ \ln\ (0.1) = -2.4\ \mathrm{kcal\ mol^{-1}},$$

and $\Delta G_t$ is −6.9 kcal mol$^{-1}$ and −6.7 kcal mol$^{-1}$ respectively for poly(dA)·poly(dT) and poly(dA-dT)·poly(dA-dT).

Similarly, the observed binding enthalpy can be parsed into two contributions:

$$\Delta H_{obs} = \Delta H_{pe} + \Delta H_t \quad (5)$$

where $\Delta H_{pe}$ is assumed to be essentially zero [53], and $\Delta H_t$ equal to $\Delta H_{obs}$. For poly(dA)·poly(dT) binding with DB75, $\Delta H_t$ was obtained as 3.1 kcal mol$^{-1}$, while for poly(dA-dT)·poly(dA-dT) binding with DB75, $\Delta H_t$ was obtained as −4.5 kcal mol$^{-1}$. From the binding free energy and enthalpy values determined above, the enthalpy ($\Delta S$) of complex formation could be calculated from Eq. (6):

$$\Delta G = \Delta H - T\Delta S. \quad (6)$$

The obtained thermodynamics parameters are summarized in Table S1. To visualize the differences of thermodynamic forces more easily, the overall thermodynamic profiles for the interaction of poly(dA)·poly(dT) and poly(dA-dT)·poly(dA-dT) with DB75 are compared in Fig. 10. As can be seen, DB75 binding to the nonalternating and alternating AT-tracts results in distinctive, sequence dependent, thermodynamic profiles.

It is worthwhile to consider what structural and property differences between alternating and nonalternating AT sequences in DNA can account for the observed differences in thermodynamics for binding DB75 and other minor groove agents. A-tract DNA is known to have a number of unusual features that distinguish it from B-form DNA as well as from other AT sequences. The minor grove of nonalternating $A_nT_n$ sequences, for example, has been shown to be more narrow than that of alternating $(AT)_n$ by solution and X-ray studies [4,54–57]. A highly ordered hydration array that can incorporate ions in the minor groove is also observed in $A_nT_n$ sequences [58–60]. A-tract

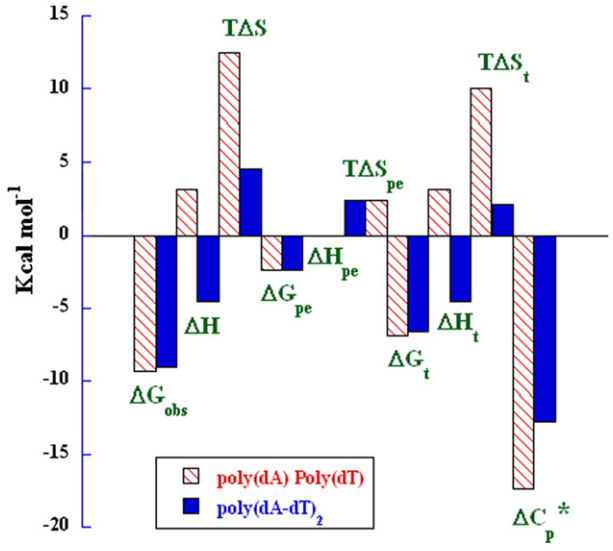


Fig. 10. Parsing the free energy ($\Delta G_{obs}$) of polymeric DNAs binding with DB75 into the contributor energy terms. The two bars on the right represent $\Delta C_p^* = \Delta C_p / 10$ in a unit of cal mol$^{-1}$ K$^{-1}$.

sequences that are in phase can cause bending of the DNA helix and this feature could be very important in cellular effects, especially in very AT rich DNAs such as the kinetoplast DNA of some eukaryotic parasites [61,62]. Ions can reach a significant concentration in A-tracts and are displaced by minor groove binding agents [63–65]. It has been proposed that such asymmetric ion binding can explain much of the curvature and narrowing of their minor groove of A-tract sequences. DNA sequences that are composed of long A-tracts also undergo a premelting transition that converts one helical form to another [66,67].

Formation of a DB75–DNA complex will result in an entropy penalty for both of the AT DNAs. To explain the significant positive entropy for DB75 binding to poly(dA)·poly (dT) requires some combination of solvent/ion release from the minor groove. It is likely that solvent release is a much more favorable contribution with poly(dA)·poly(dT) than with poly (dA-dT)·poly(dA-dT) due to the more highly ordered groove solvation in the nonalternating sequence [68]. Release of highly ordered water on binding to the minor groove can also result in a significant enthalpy penalty which can account for the positive binding enthalpy for DB75 with poly(dA)·poly(dT) (Fig. 10). Binding to poly(dA-dT)·poly(dA-dT) would then appear to be more typical of AT DNA sequences in general and to involve a combination of favorable enthalpy terms for compound–DNA interactions, favorable entropy from ordered water/ion release, but unfavorable terms for disruption of water–DNA interactions and the entropy of compound binding. For compounds such as DB75 that match the curvature and functional group placement in the AT minor groove, this results in a favorable Gibbs energy for DNA complex formation in AT sequences.

Observations that would appear to contrast with this explanation involve osmotic stress measurements of DNA–small molecule binding that indicate a net water uptake, not release, on complex formation [69–71]. This requires reconciliation of the generally observed positive entropy for AT minor groove binding with water uptake on complex formation. A possible explanation for these apparently contradictory findings would involve two types of water exchange in the binding process. Highly ordered, high entropy water that is released from the minor groove in the binding reaction would dominate the entropy term while a larger amount of relatively unstructured, highly mobile, low entropy water could become associated with the DNA complex. The net binding entropy would be positive in this situation while the net amount of bound water would increase. The more highly structured the water that is released, as from the groove of poly(dA)·poly(dT), the more dominant the entropy of binding term would become to the Gibbs energy of complex formation.

The $\Delta C_p$ value for DB75 binding to both AT polymers is negative (Fig. 10), in agreement with results for other similar minor groove binding cations [70,72] and as observed in many biological conformational changes and interactions [73]. The $\Delta C_p$ for the alternating polymer is close to the value observed for DB75 binding to the –AATT- site in a duplex oligomer [47] and is slightly less than the value obtained with poly(dA)·poly (dT). As with the $\Delta S$ and $\Delta H$ of binding discussed above, there are several possible important contributions to the $\Delta C_p$ for DB75 binding to the AT polymers. Structured water release is expected to be an important contribution to $\Delta C_p$ and the $\Delta C_p$ values in Fig. 10 are close to the predicted values based on changes in solvent accessible surface area on binding. These values are calculated based on an equation from Chaires and coworkers [36] from experimental results for small molecule–DNA experiments. The slightly larger value of $\Delta C_p$ for DB75 binding to poly(dA)·poly(dT) could come from disruption of a larger ordered water network in the minor grove of that polymer relative to poly(dA-dT)·poly(dA-dT). Loss of some dynamic capability, soft vibrational modes, as well as other contributions could also lead a negative $\Delta C_p$ on binding of DB75 [74].

In summary, CD studies with alternating and nonalternating AT DNA sequences of varying length provide strong evidence that DB75 binds tightly in the minor groove of all of the AT sites. Unlike minor grove binding, organic cations in general, both Tm and SPR results show that DB75 has similar binding constants with the alternating and nonalternating AT sequences. ITC results with the different AT sequences, however, clearly demonstrate that the thermodynamics underlying the $\Delta G$ value for binding are completely different. The differences in $\Delta H$, $\Delta S$ and $\Delta C_p$ on binding to the two DNAs are summarized in Fig. 10. These differences can be explained by a combination of effects that involve differences in amount and order of water release from the minor groove as well as moderate conformational changes on DB75 binding. These differences in thermodynamics are DNA sequence related and it is highly likely that similar findings will be observed for many minor groove binding agents.

## Acknowledgments

This research was supported by the National Institutes of Health Grants GM61587 and AI064200 (to WDW and DWB) and equipment purchases were partially funded by the Georgia Research Alliance.

## Appendix A. Supplementary data

Supplementary data associated with this article can be found, in the online version, at doi:10.1016/j.bpc.2007.08.007.

## References


[1] A.J. Hampshire, D.A. Rusling, V.J. Broughton-Head, K.R. Fox, Footprinting: a method for determining the sequence selectivity, affinity and kinetics of DNA-binding ligands, Methods (S. Diego Calif.) 42 (2007) 128–140.

[2] C. Bailly, J.B. Chaires, Sequence-specific DNA minor groove binders. Design and synthesis of netropsin and distamycin analogues, Bioconjug. Chem. 9 (1998) 513–538.

[3] S.A. Weston, A. Lahm, D. Suck, X-ray structure of the DNase I-d $(GGTATACC)_2$ complex at 2.3 A resolution, J. Mol. Biol. 226 (1992) 1237–1256.

[4] A. Abu-Daya, P.M. Brown, K.R. Fox, DNA sequence preferences of several AT-selective minor groove binding ligands, Nucleic Acids Res. 23 (1995) 3385–3392.

[5] A. Abu-Daya, K.R. Fox, Interaction of minor groove binding ligands with long AT tracts, Nucleic Acids Res. 25 (1997) 4962–4969.

[6] C. Zimmer, Effects of the antibiotics netropsin and distamycin A on the structure and function of nucleic acids, Prog. Nucleic Acid Res. Mol. Biol. 15 (1975) 285–318.

[7] C. Zimmer, C. Marck, C. Schneider, W. Guschlbauer, Influence of nucleotide sequence on dA·dT-specific binding of Netropsin to double stranded DNA, Nucleic Acids Res. 6 (1979) 2831–2837.

[8] P.B. Dervan, R.W. Burli, Sequence-specific DNA recognition by polyamides, Curr. Opin. Chem. Biol. 3 (1999) 688–693.

[9] Z. Moravek, S. Neidle, B. Schneider, Protein and drug interactions in the minor groove of DNA, Nucleic Acids Res. 30 (2002) 1182–1191.

[10] S. Neidle, DNA minor-groove recognition by small molecules, Nat. Prod. Rep. 18 (2001) 291–309.

[11] B.S. Reddy, S.M. Sondhi, J.W. Lown, Synthetic DNA minor groove-binding drugs, Pharmacol. Ther. 84 (1999) 1–111.

[12] D.E. Wemmer, P.B. Dervan, Targeting the minor groove of DNA, Curr. Opin. Struct. Biol. 7 (1997) 355–361.

[13] C. Bailly, M.J. Waring, Use of DNA molecules substituted with unnatural nucleotides to probe specific drug–DNA interactions, Methods Enzymol. 340 (2001) 485–502.

[14] S.Y. Breusegem, R.M. Clegg, F.G. Loontiens, Base-sequence specificity of Hoechst 33258 and DAPI binding to five $(A/T)_4$ DNA sites with kinetic evidence for more than one high-affinity Hoechst 33258-AATT complex, J. Mol. Biol. 315 (2002) 1049–1061.

[15] N.V. Hud, M. Polak, DNA–cation interactions: The major and minor grooves are flexible ionophores, Curr. Opin. Struck. Biol. 11 (2001) 293–301.

[16] E. Johansson, G. Parkinson, S. Neidle, A new crystal form for the dodecamer C-G-C-G-A-A-T-T-C-G-C-G: symmetry effects on sequence-dependent DNA structure, J. Mol. Biol. 300 (2000) 551–561.

[17] K.K. Woods, T. Maehigashi, S.B. Howerton, C.C. Sines, S. Tannenbaum, L.D. Williams, High-resolution structure of an extended A-tract: $[d(CGCAAATTTGCG)]_2$, J. Am. Chem. Soc. 126 (2004) 15330–15331.

[18] N.V. Hud, J. Plavec, A unified model for the origin of DNA sequence-directed curvature, Biopolymers 69 (2003) 144–158.

[19] R.R. Tidwell, D.W. Boykin, In DNA and RNA binders: from small molecules to drugs, in: M. Demeunynck, C. Bailly, W.D. Wilson (Eds.), Wiley-VCH, 2003, pp. 414–460.

[20] A.M. Mathis, A.S. Bridges, M.A. Ismail, A. Kumar, I. Francesconi, M. Anbazhagan, Q. Hu, F.A. Tanious, T. Wenzler, J. Saulter, W.D. Wilson, R. Brun, D.W. Boykin, R.R. Tidwell, J.E. Hall, Diphenyl furans and Aza Analogs: effects of structural modification on in vitro activity, DNA binding, and accumulation and distribution in trypanosomes, Antimicrob. Agents Chemother. 51 (2007) 2801–2810.

[21] D.W. Boykin, Antimicrobial activity of the DNA minor groove binders furamidine and analogs, J. Braz. Chem. Soc. 13 (2002) 763–771.

[22] W.D. Wilson, B. Nguyen, F.A. Tanious, A. Mathis, J.E. Hall, C.E. Stephens, D.W. Boykin, Dications that target the DNA minor groove: compound design and preparation, DNA interactions, cellular distribution and biological activity, Curr. Med. Chem. Anti-cancer Agents 5 (2005) 389–408.

[23] T. Cui, S. Wei, K. Brew, F. Leng, Energetics of binding the mammalian high mobility group protein HMGA2 to poly(dA-dT)$_2$ and poly(dA)–poly (dT), J. Mol. Biol. 352 (2005) 629–645.

[24] L.A. Marky, K.J. Breslauer, Origins of netropsin binding affinity and specificity: correlations of thermodynamic and structural data, Proc. Natl. Acad. Sci. U. S. A. 84 (1987) 4359–4363.

[25] X. Shi, R.B. Macgregor Jr., Temperature dependence of the volumetric parameters of drug binding to poly[d(A-T)]·Poly[d(A-T)] and Poly (dA)·Poly(dT), Biophys. J. 90 (2006) 1729–1738.

[26] B. Liu, Y. Liu, S.A. Motyka, E.E. Agbo, P.T. Englund, Fellowship of the rings: the replication of kinetoplast DNA, Trends Parasitol. 21 (2005) 363–369.

[27] J. Lukes, D.L. Guilbride, J. Votypka, A. Zikova, R. Benne, P.T. Englund, Kinetoplast DNA network: evolution of an improbable structure, Eukaryot. Cell. 1 (2002) 495–502.

[28] T.A. Shapiro, P.T. Englund, The structure and replication of kinetoplast DNA, Annu. Rev. Microbiol. 49 (1995) 117–143.

[29] M. Hong, L. Simpson, Genomic organization of *Trypanosoma brucei* kinetoplast DNA minicircles, Protist 154 (2003) 265–279.

[30] J.B. Chaires, J. Ren, D. Hamelberg, A. Kumar, V. Pandya, D.W. Boykin, W.D. Wilson, Structural selectivity of aromatic diamidines, J. Med. Chem. 47 (2004) 5729–5742.

[31] B.P. Das, D.W. Boykin, Synthesis and antiprotozoal activity of 2,5-bis(4-guanylphenyl)furans, J. Med. Chem. 20 (1977) 531–536.

[32] J.F. Brandts, L.N. Lin, Study of strong to ultratight protein interactions using differential scanning calorimetry, Biochemistry 29 (1990) 6927–6940.

[33] K.J. Breslauer, Extracting thermodynamic data from equilibrium melting curves for oligonucleotide order–disorder transitions, Methods Enzymol. 259 (1995) 221–242.

[34] F. Leng, W. Priebe, J.B. Chaires, Ultratight DNA binding of a new bisintercalating anthracycline antibiotic, Biochemistry 37 (1998) 1743–1753.

[35] F. Barcelo, D. Capo, J. Portugal, Thermodynamic characterization of the multivalent binding of chartreusin to DNA, Nucleic Acids Res. 30 (2002) 4567–4573.

[36] J. Ren, T.C. Jenkins, J.B. Chaires, Energetics of DNA intercalation reactions, Biochemistry 39 (2000) 8439–8447.

[37] B. Nguyen, F.A. Tanious, W.D. Wilson, Biosensor-surface plasmon resonance: quantitative analysis of small molecule-nucleic acid interactions, Methods (S. Diego Calif.) 42 (2007) 150–161.

[38] T.M. Davis, W.D. Wilson, Determination of the refractive index increments of small molecules for correction of surface plasmon resonance data, Anal. Biochem. 284 (2000) 348–353.

[39] A.N. Lane, T.C. Jenkins, T. Brown, S. Neidle, Interaction of berenil with the EcoRI dodecamer d$(CGCGAATTCGCG)_2$ in solution studied by NMR, Biochemistry 30 (1991) 1372–1385.

[40] A.B. Malin, N. Tomas, K., Circular Dichroism, in: B. Nina, N. Koji, W. Roberts (Eds.), Wiley-VCH, 2000, pp. 741–768.

[41] K.J. Breslauer, D.P. Remeta, W.Y. Chou, R. Ferrante, J. Curry, D. Zaunczkowski, J.G. Snyder, L.A. Marky, Enthalpy–entropy compensations in drug–DNA binding studies, Proc. Natl. Acad. Sci. U. S. A. 84 (1987) 8922–8926.

[42] J.B. Chaires, Energetics of drug–DNA interactions, Biopolymers 44 (1997) 201–215.

[43] I. Midgley, K. Fitzpatrick, L.M. Taylor, T.L. Houchen, S.J. Henderson, S.J. Wright, Z.R. Cybulski, B.A. John, A. McBurney, D.W. Boykin, K.L. Trendler, Pharmacokinetics and metabolism of the prodrug DB289 (2,5-bis [4-(*N*-methoxyamidino)phenyl]furan monomaleate) in rat and monkey and its conversion to the antiprotozoal/antifungal drug DB75 (2,5-bis(4-guanylphenyl)furan dihydrochloride), Drug Metab. Dispos. 35 (2007) 955–967.

[44] M.L. Stewart, S. Krishna, R.J. Burchmore, R. Brun, H.P. de Koning, D.W. Boykin, R.R. Tidwell, J.E. Hall, M.P. Barrett, Detection of arsenical drug

resistance in *Trypanosoma brucei* with a simple fluorescence test, Lancet 366 (2005) 486–487.
[45] K.L. Buchmueller, A.M. Staples, C.M. Howard, S.M. Horick, P.B. Uthe, N.M. Le, K.K. Cox, B. Nguyen, K.A. Pacheco, W.D. Wilson, M. Lee, Extending the language of DNA molecular recognition by polyamides: unexpected influence of imidazole and pyrrole arrangement on binding affinity and specificity, J. Am. Chem. Soc. 127 (2005) 742–750.
[46] E.R. Lacy, N.M. Le, C.A. Price, M. Lee, W.D. Wilson, Influence of a terminal formamido group on the sequence recognition of DNA by polyamides, J. Am. Chem. Soc. 124 (2002) 2153–2163.
[47] S. Mazur, F.A. Tanious, D. Ding, A. Kumar, D.W. Boykin, I.J. Simpson, S. Neidle, W.D. Wilson, A thermodynamic and structural analysis of DNA minor-groove complex formation, J. Mol. Biol. 300 (2000) 321–337.
[48] C.M. Nunn, S. Neidle, Sequence-dependent drug binding to the minor groove of DNA: crystal structure of the DNA dodecamer $d(CGCAAATTTGCG)_2$ complexed with propamidine, J. Med. Chem. 38 (1995) 2317–2325.
[49] J. Lah, G. Vesnaver, Energetic diversity of DNA minor-groove recognition by small molecules displayed through some model ligand–DNA systems, J. Mol. Biol. 342 (2004) 73–89.
[50] J.B. Chaires, Dissecting the free energy of drug binding to DNA, Anticancer Drug Des. 11 (1996) 569–580.
[51] I. Haq, Thermodynamics of drug–DNA interactions, Arch. Biochem. Biophys. 403 (2002) 1–15.
[52] M.T. Record Jr., C.F. Anderson, T.M. Lohman, Thermodynamic analysis of ion effects on the binding and conformational equilibria of proteins and nucleic acids: the roles of ion association or release, screening, and ion effects on water activity, Q. Rev. Biophys. 11 (1978) 103–178.
[53] M.M. Patel, T.J. Anchordoquy, Contribution of hydrophobicity to thermodynamics of ligand–DNA binding and DNA collapse, Biophys. J. 88 (2005) 2089–2103.
[54] H.M. Berman, Crystal studies of B-DNA: the answers and the questions, Biopolymers 44 (1997) 23–44.
[55] G.L. Olsen, E.A. Louie, G.P. Drobny, S.T. Sigurdsson, Determination of DNA minor groove width in distamycin–DNA complexes by solid-state NMR, Nucleic Acids Res. 31 (2003) 5084–5089.
[56] K.R. Fox, Probing the conformations of eight cloned DNA dodecamers; CGCGAATTCGCG, CGCGTTAACGCG, CGCGTATACGCG, CGCGATATCGCG, CGCAAATTTGCG, CGCTTTAAAGCG, CGCGGATCCGCG and CGCGGTACCGCG, Nucleic Acids Res. 20 (1992) 6487–6493.
[57] C. Bailly, N.E. Mollegaard, P.E. Nielsen, M.J. Waring, The influence of the 2-amino group of guanine on DNA conformation. Uranyl and DNase I probing of inosine/diaminopurine substituted DNA, EMBO J. 14 (1995) 2121–2131.
[58] D. Hamelberg, L.D. Williams, W.D. Wilson, Influence of the dynamic positions of cations on the structure of the DNA minor groove: sequence-dependent effects, J. Am. Chem. Soc. 123 (2001) 7745–7755.
[59] S.B. Howerton, C.C. Sines, D. VanDerveer, L.D. Williams, Locating monovalent cations in the grooves of B-DNA, Biochemistry 40 (2001) 10023–10031.
[60] L.D. Williams, L.J. Maher III, Electrostatic mechanisms of DNA deformation, Annu. Rev. Biophys. Biomol. Struct. 29 (2000) 497–521.
[61] S.D. Levene, H.M. Wu, D.M. Crothers, Bending and flexibility of kinetoplast DNA, Biochemistry 25 (1986) 3988–3995.
[62] J.C. Marini, S.D. Levene, D.M. Crothers, P.T. Englund, Bent helical structure in kinetoplast DNA, Proc. Natl. Acad. Sci. U. S. A. 79 (1982) 7664–7668.
[63] F. Cesare Marincola, V.P. Denisov, B. Halle, Competitive Na(+) and Rb(+) binding in the minor groove of DNA, J. Am. Chem. Soc. 126 (2004) 6739–6750.
[64] V.P. Denisov, B. Halle, Sequence-specific binding of counterions to B-DNA, Proc. Natl. Acad. Sci. U. S. A. 97 (2000) 629–633.
[65] B. Halle, V.P. Denisov, Water and monovalent ions in the minor groove of B-DNA oligonucleotides as seen by NMR, Biopolymers 48 (1998) 210–233.
[66] S.S. Chan, K.J. Breslauer, M.E. Hogan, D.J. Kessler, R.H. Austin, J. Ojemann, J.M. Passner, N.C. Wiles, Physical studies of DNA premelting equilibria in duplexes with and without homo dA·dT tracts: correlations with DNA bending, Biochemistry 29 (1990) 6161–6171.
[67] J.E. Herrera, J.B. Chaires, A premelting conformational transition in poly (dA)–Poly(dT) coupled to daunomycin binding, Biochemistry 28 (1989) 1993–2000.
[68] X. Shui, L. McFail-Isom, G.G. Hu, L.D. Williams, The B-DNA dodecamer at high resolution reveals a spine of water on sodium, Biochemistry 37 (1998) 8341–8355.
[69] N.N. Degtyareva, B.D. Wallace, A.R. Bryant, K.M. Loo, J.T. Petty, Hydration changes accompanying the binding of minor groove ligands with DNA, Biophys. J. 92 (2007) 959–965.
[70] J.R. Kiser, R.W. Monk, R.L. Smalls, J.T. Petty, Hydration changes in the association of Hoechst 33258 with DNA, Biochemistry 44 (2005) 16988–16997.
[71] X. Qu, J.B. Chaires, Hydration changes for DNA intercalation reactions, J. Am. Chem. Soc. 123 (2001) 1–7.
[72] I. Haq, J.E. Ladbury, B.Z. Chowdhry, T.C. Jenkins, J.B. Chaires, Specific binding of Hoechst 33258 to the $d(CGCAAATTTGCG)_2$ duplex: calorimetric and spectroscopic studies, J. Mol. Biol. 271 (1997) 244–257.
[73] A. Cooper, Heat capacity effects in protein folding and ligand binding: a re-evaluation of the role of water in biomolecular thermodynamics, Biophys. Chemist. 115 (2005) 89–97.
[74] J.M. Sturtevant, Heat capacity and entropy changes in processes involving proteins, Proc. Natl. Acad. Sci. U. S. A. 74 (1977) 2236–2240.